Atmos. Chem. Phys., 17, 5865–5876, 2017
www.atmos-chem-phys.net/17/5865/2017/
doi:10.5194/acp-17-5865-2017

Atmospheric Chemistry and Physics Open Access EGU

How does sea ice influence $\delta^{18}O$ of Arctic precipitation?

Anne-Katrine Faber[1], Bo Møllesøe Vinther[1], Jesper Sjolte[2], and Rasmus Anker Pedersen[1,3]

[1]Centre for Ice and Climate, Niels Bohr Institute, University of Copenhagen, Copenhagen, Denmark
[2]Department of Geology, Quaternary Sciences, Lund University, Lund, Sweden
[3]Climate and Arctic Research, Danish Meteorological Institute, Copenhagen, Denmark

Correspondence to: Anne-Katrine Faber (anne-katrine.faber@uib.no)

Received: 1 February 2016 – Discussion started: 14 March 2016
Revised: 12 August 2016 – Accepted: 15 August 2016 – Published: 12 May 2017

Abstract. This study investigates how variations in Arctic sea ice and sea surface conditions influence $\delta^{18}O$ of present-day Arctic precipitation. This is done using the model isoCAM3, an isotope-equipped version of the National Center for Atmospheric Research Community Atmosphere Model version 3. Four sensitivity experiments and one control simulation are performed with prescribed sea surface temperature (SST) and sea ice. Each of the four experiments simulates the atmospheric and isotopic response to Arctic oceanic conditions for selected years after the beginning of the satellite era in 1979.

Changes in sea ice extent and SSTs have different impacts in Greenland and the rest of the Arctic. The simulated changes in central Arctic sea ice do not influence $\delta^{18}O$ of Greenland precipitation, only anomalies of Baffin Bay sea ice. However, this does not exclude the fact that simulations based on other sea ice and sea surface temperature distributions might yield changes in the $\delta^{18}O$ of precipitation in Greenland. For the Arctic, $\delta^{18}O$ of precipitation and water vapour is sensitive to local changes in sea ice and sea surface temperature and the changes in water vapour are surface based. Reduced sea ice extent yields more enriched isotope values, whereas increased sea ice extent yields more depleted isotope values. The distribution of the sea ice and sea surface conditions is found to be essential for the spatial distribution of the simulated changes in $\delta^{18}O$.

1 Introduction

Records of stable water isotopologues from polar ice cores have been widely used to reconstruct past climate variability. Since the pioneering work by Dansgaard (1964), the understanding of stable water isotopologues as a proxy for temperature has significantly advanced. It has become clear that the isotopic composition of precipitation is a complex signal, influenced by both local and regional climate conditions (Vinther et al., 2010; Steen-Larsen et al., 2011; Sjolte et al., 2011; Sodemann et al., 2008b; White et al., 1997; Johnsen et al., 1989). The isotopic composition of the precipitation is an integrated signal of the conditions along the moisture transport pathway from source to deposition. As a result, there is a need for a detailed process-based understanding of the factors that can alter the isotopic composition of the transported moisture.

Studies using models, ice cores, snow and water vapour measurements have investigated the physical and dynamical processes influencing the isotopic composition of precipitation. Variations in local Greenland temperatures, conditions at source regions and atmospheric circulation all influence the isotopic composition of Greenland precipitation (Steen-Larsen et al., 2011; Bonne et al., 2014; Sodemann et al., 2008a, b; Sjolte et al., 2011; Vinther et al., 2010).

Several model studies highlight sea ice changes as important for understanding changes in the isotopic composition of precipitation. Sea ice changes in the Arctic were investigated during Dansgaard–Oeschger events (Li et al., 2010) and for exceptionally warm climates (Sime et al., 2013). For Antarctica, the impact of sea ice changes were studied using idealized reductions of the circular shaped sea ice cover (Noone, 2004). None of these model studies investigate sea ice per-

turbation comparable to present-day observations. Measurements from ice cores spanning this period suggest that sea ice changes can influence the isotopic composition of precipitation (Divine et al., 2011; Opel et al., 2013; Ku et al., 2012; Fauria et al., 2010).

A study of idealised changes of Antarctic sea ice showed a non-uniform spatial distribution of the modelled isotopic response over Antarctica (Noone, 2004). The heterogeneity of the response is suggested to reflect the existence of different processes driving local and long range moisture transport to coastal and high elevation regions of Antarctica. Due to differences in the configuration of landmasses, open ocean and sea ice, it is difficult to directly transfer findings of Noone (2004) from Antarctic to the Arctic.

The impact of changes in sea ice and connected sea surface temperatures (SSTs) of the Arctic ocean were studied by Sime et al. (2013). The sea ice conditions were created using an experiment where a coupled climate model was forced by respectively $2\times$, $4\times$ and $8\times CO_2$. Subsequently the sea ice and SST conditions were used to force the applied atmospheric isotope models. Differences in the configurations of sea ice extent and SST were found to be essential for the resulting large variability in the isotope–temperature slope of 0.1–0.7 ‰ °C^{-1} for the Greenland Ice Sheet. While these CO_2 changes used by Sime et al. (2013) do not allow direct comparison with present-day Arctic conditions, the results highlight processes that might be important for present-day climate.

The recent decades of rapid Arctic sea ice decline provides an interesting opportunity to study how δ^{18}O responds to realistic changes of sea ice and SSTs of present-day climate. Here we present results from isoCAM3 model simulations forced with observed Arctic sea ice and SST conditions derived from observations. This paper will address how the sea ice and sea surface conditions influence the δ^{18}O of precipitation in the Arctic, and the role of the spatial configuration of sea surface changes. The structure of the paper is as follows: (1) the model and experiments are described, (2) results of the simulations are presented and (3) the influence of atmospheric moisture processes is discussed.

2 Experimental configuration

2.1 The model isoCAM3

The simulations of the isotopic composition of precipitation and water vapour in this study are conducted with isoCAM3. This is an atmospheric general circulation model (AGCM) enabled with the ability to trace the various species of water isotopologues. The model is based on the Community Atmosphere Model version 3 (CAM3) (Collins et al., 2006), and the isotope module was developed by David Noone, University of Colorado. More details of isoCAM3 can be found in Noone and Sturm (2010) The isoCAM3 model has been applied in several studies that investigated the isotopic response to past climate changes (Tharammal et al., 2013; Speelman et al., 2010; Sturm et al., 2010; Pausata et al., 2011; Liu et al., 2012; Sewall and Fricke, 2013; Liu et al., 2014).

The horizontal resolution of the model is T85 ($\sim 1.4^\circ \times 1.4^\circ$) with 26 hybrid-sigma levels in the vertical. In this study the SST and sea ice concentrations are specified; thus, the only surface temperatures that are calculated interactively are land and sea ice surface temperatures. This configuration allows for no feedback between atmospheric circulation and open-ocean SST. Greenhouse gases, vegetation, ice sheets are all set to modern conditions. More specifically greenhouse gasses are set to the following CAM3 default levels (year 1990): CO_2 – 355 (ppmv), CH_4 – 1714 (ppbv), N_2O – 311 (ppbv). The solar constant is set to 1365 (W m^{-2}) and orbital configurations are set to the year 1850.

2.2 Ensemble design

We perform a set of four sensitivity experiments and one control simulation to investigate how observed variations in Arctic sea surface conditions influences δ^{18}O. Every model integration is run for 15 years (following 1 year for spin-up). Each of the four sensitivity experiments simulates the δ^{18}O response to sea ice concentration and SST for selected years in the time period 1979–2013 within the satellite era. The 12-month time periods are selected based on the four most extreme cases of high and low September sea ice extent recorded during the time period (1979–2012) by the National Snow and Ice Data Center (NSIDC) Sea Ice Index (Fetterer et al., 2002, updated daily). The control simulation (CTRL) simulates the δ^{18}O response using the 12-month climatology of sea ice concentration and SST for the full time period April 1979–March 2013. Only the Arctic oceanic surface boundary conditions differ between the runs. An overview of the model experiments are given in Table 1.

We force the model isoCAM3 with an annual cycle of monthly mean SST and sea ice conditions obtained from ERA-Interim (Dee et al., 2011). This annual cycle goes from April to March, thus spanning the full sea ice cycle related to the selected cases of September sea ice extent. Subsequently, the model runs for 15 years (following 1 year of spin-up) with repeated annual cycles. All re-analysis data are interpolated bilinearly from the ERA-Interim ($1^\circ \times 1^\circ$) to the CAM3 T85 resolution, and subsequently checked for consistency.

Changes in Arctic SST are in nature an inseparable part of sea ice changes. Keeping the SST constant and only simulating the atmospheric response to sea ice changes, would therefore lead to unrealistic temperature gradients (see Screen et al., 2013b, for further discussion on this topic). Therefore, we chose that these experiments are based on both changes in sea ice and SST. A masking of the SST data is applied to eliminate remote influences from extra-polar climate pat-

Table 1. Overview of model experiments.

Experiment	Prescribed SST and sea ice
"1980"	ERA-Interim monthly mean: April 1980–March 1981
"1996"	ERA-Interim monthly mean: April 1996–March 1997
"2007"	ERA-Interim monthly mean: April 2007–March 2008
"2012"	ERA-Interim monthly mean: April 2012–March 2013
CTRL	ERA-Interim monthly mean climatology: April 1979–March 2013

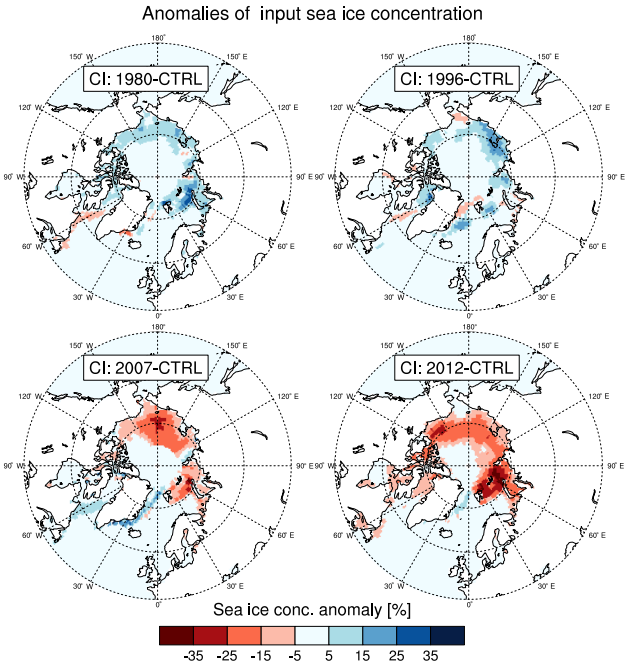

Figure 1. Annual mean anomalies of sea ice concentration (CI) used to force the model. See Table 1 for details. Red colours represent a decrease in sea ice compared to the CTRL run. Blue colours represent an increase in sea ice compared to the CTRL run (mean April 1979 to March 2013).

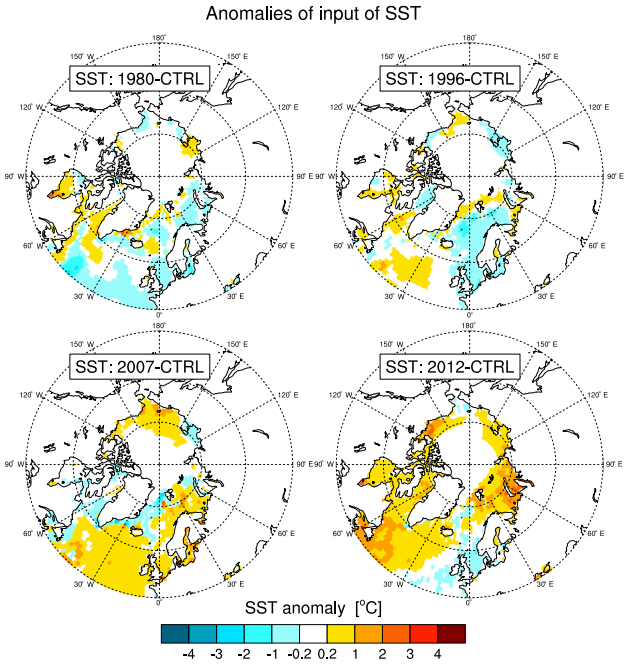

Figure 2. Annual mean anomalies of sea surface temperature (SST) used to force the model. See Table 1 for details. Red and yellow colours represent an increase in SST compared to the CTRL run. Blue colours represent a decrease in SST compared to the CTRL run (mean April 1979 to March 2013).

terns (e.g. from the El Niño–Southern Oscillation or Pacific Decadal Oscillation). This masking is constructed so that only the conditions near the Arctic differ from experiment to experiment. Hence, this global ocean data are divided in an Arctic and a non-Arctic region. The Arctic region refers to the region of ocean/sea ice conditions expected to influence the Arctic climate and is therefore rather semi-Arctic. Due the geographical configuration of the continents it is chosen to confine this region with southern boundaries of 66° and 37° N for the Pacific and Atlantic sector respectively. The relatively southern definition of the semi-Arctic region in the North Atlantic is chosen to also include the southern-most position of sea ice export in the Newfoundland area.

Each experiment is forced by different SST and sea ice conditions in the (semi-)Arctic region corresponding to the values for the selected year. The non-Arctic part of the data set is identical for all the different experiments and has values from the mean climatology of ERA-Interim 1979–2012. The area between the Arctic and non-Arctic part in the North Atlantic has strong naturally occurring SST gradients. To avoid smoothing of natural SST gradients, no smoothing is applied to the constructed oceanic data set. The sea ice concentrations and SST used to force the model are shown in Figs. 1 and 2 here displayed as annual mean anomalies between the respective experiment and the CTRL run.

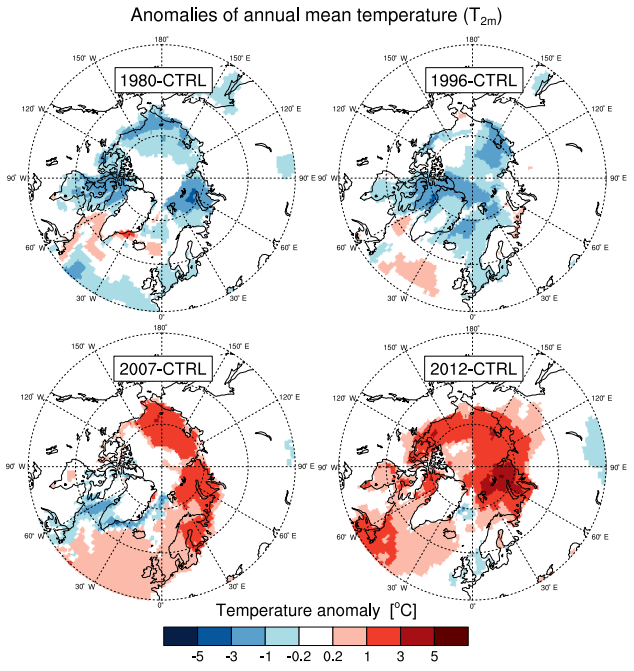

Figure 3. Annual mean anomalies of surface air temperatures ($T_{2\,\mathrm{m}}$). Annual mean anomalies for the four simulations compared to the CTRL run. Red colours represent a increase in $T_{2\,\mathrm{m}}$ compared to the CTRL run. Blue colours represent a decrease in $T_{2\,\mathrm{m}}$ compared to the CTRL run Only anomalies statistically significant at the 95 % confidence level are shown.

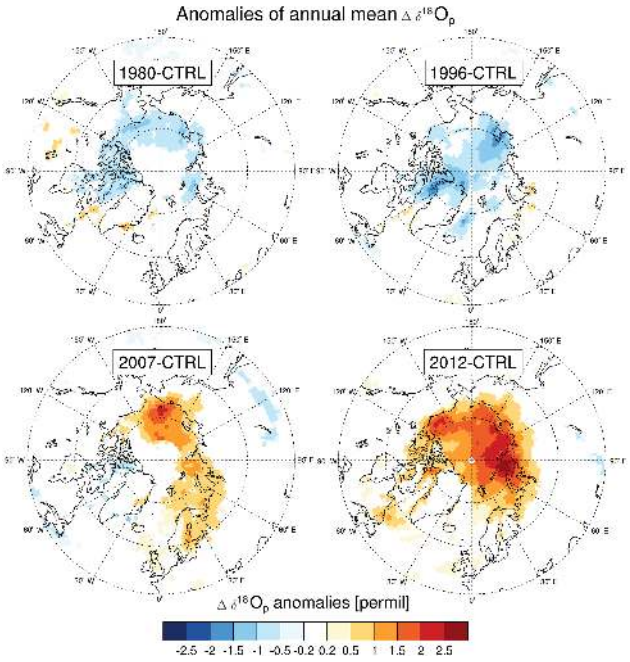

Figure 4. Annual mean anomalies of δ^{18}O of precipitation ($\delta^{18}O_p$). Annual mean anomalies for the four simulations compared to the CTRL run. Only anomalies statistically significant at the 95 % confidence level are shown. Red and yellow colours represent an increase in $\delta^{18}O_p$ compared to the CTRL run. Blue colours represent a decrease in $\delta^{18}O_p$ compared to the CTRL run.

3 Atmospheric response to changes in sea ice extent

3.1 Atmospheric response

Changes in sea ice concentration and SST force a strong local response in surface air temperature ($T_{2\,\mathrm{m}}$) (see Fig. 3) with cooling where sea ice extent is increased, and warming where sea ice extent is decreased. The simulated temperature changes are in agreement with other modelling studies that have investigated the atmospheric response to prescribed reanalysis-based changes (Screen et al., 2013a; Magnusdottir et al., 2004; Blüthgen et al., 2012, see also reviews Budikova, 2009; Bader et al., 2011). Changes in annual mean precipitation amount are found negligible (see Appendix A).

3.2 Isotopic response

The CTRL run is compared to values of δ^{18}O observations from ice cores and GNIP stations for Greenland and a positive bias is found (see figure in Appendix A). As a consequence this study only investigates anomalies and not absolute values. All sensitivity experiments clearly show that changes in sea surface conditions influence the modelled δ^{18}O of Arctic precipitation (Fig. 4). Decreased (increased) sea ice concentration and connected SST results in enriched (depleted) δ^{18}O values of precipitation (hereafter referred to as $\delta^{18}O_p$). Annual means of $\delta^{18}O_p$ are computed as precipitation-weighted annual means. The spatial distribution of changes in $\delta^{18}O_p$ is similar to the spatial distribution of changes in simulated surface air temperature.

This shows that the spatial response of the simulated $\delta^{18}O_p$ to changes in sea surface conditions is controlled by the distribution of these changes. The distribution of the $\delta^{18}O_p$ response to the ocean conditions depends on the sea ice and SST configuration in the different experiments. As shown in Fig. 4 the $\delta^{18}O_p$ of the precipitation over central part of Greenland appears unaffected by the simulated changes in sea ice cover in all experiments whereas $\delta^{18}O_p$ changes over the Pacific–Arctic oceans and the Barents–Kara seas regions depend on the distribution of sea ice in the given experiment.

The experiments "1980" and "1996" both have increased sea ice extent and colder SSTs compared to the CTRL experiments, yet the spatial distributions of the sea surface conditions in the Arctic Ocean are very different. This is observed in the Barents/Kara Sea region, in Baffin Bay and near the northern coast of Greenland. The corresponding isotopic response match the differences in the spatial pattern observed in the sea ice cover.

The two experiments with low sea ice extent compared to the CTRL experiments (the "2007" and "2012" experiments) similarly show that the sea ice distribution is important for

$\delta^{18}O_p$. The Labrador–Baffin seas region does not experience any significant change in the isotopic composition of precipitation in the "2007" experiment. Conversely, significant changes are simulated in the "2012" experiment where the sea ice changes in this region are much more pronounced. For the Barents Sea region both experiments yield positive $\delta^{18}O_p$ anomalies, but the amplitude of the anomalies are different. Interestingly, this difference in amplitudes is also found in the sea ice concentration anomalies used to simulate the isotopic response. Thus, this suggests that both distribution and magnitude of the changes in sea surface conditions are important for the change in $\delta^{18}O_p$.

3.3 $\delta^{18}O_p$-temperature relationship

From a climate reconstruction perspective it is interesting to examine whether the isotope-temperature relationship ($\delta^{18}O_p$–T) is sensitive to changes in sea ice cover and SST. Scatter plots of annual mean anomalies of $\Delta\delta^{18}O_p$–ΔT are shown in Fig. 5. Only grid points in the Arctic (60–90° N) are included in the analysis.

Linear regression shows that the spatial $\Delta\delta^{18}O_p$–ΔT slopes for each of the experiment all are within the range of 0.38 to 0.53 ‰ °C^{-1}. Linear regression for all experiments together (Fig. 5 "All experiments") show a larger range of values of anomalies and yields a slope of 0.57 ‰ °C^{-1} with $R^2 = 0.761$. For experiments with high sea ice extent, the slope is 0.38 ‰ °C^{-1} with $R^2 = 0.59$ for "1980" and 0.53 ‰ °C^{-1} with $R^2 = 0.575$ for "1996". For experiments with low sea ice extent, the value of the slope is 0.42 ‰ °C^{-1} with $R^2 = 0.732$ for "2007" and 0.48 ‰ °C^{-1} with $R^2 = 0.635$ for "2012".

In this study, the slope of $\delta^{18}O_p$–T relationship is found to be insensitive to changes in the perturbation of sea ice. Differences in the intercept values of the regression are noted, most pronounced for experiment "2012" where the offset of $\Delta\delta^{18}O_p$ is −0.39 ‰.

3.4 Atmospheric moisture processes

The $\delta^{18}O_p$ response to sea ice changes (Fig. 4) shows that the response is predominantly local, yet with the "2012" experiment showing a more regional response. Here we broadly define a local response as a situation where the grid points in close proximity to regions of sea ice change experience large changes in $\delta^{18}O_p$, and where grid points without sea ice change show no pronounced changes in $\delta^{18}O_p$. Similarly, a regional response here is used to describe a response where changes in $\delta^{18}O_p$ both occur at grid points in close proximity to regions of sea ice changes and also at neighbouring grid points without sea ice changes.

Examination of the anomalies of isotopic composition of the water vapour yields insight into the isotopic composition of the Arctic moisture. Figure 6 shows the anomaly of isotopic water vapour composition at the 850 hPa level (hereafter referred to as $\delta^{18}O_v$). The anomaly is plotted with the 850 hPa level wind field anomaly overlayed. Similar to the isotopic composition of precipitation, the isotopic composition of water vapour at the 850 hPa level reveals, for all experiments, local anomalies at the same locations as anomalies of sea surface conditions occur. Locations with decreased (increased) sea ice extent and concentration are co-located with locations of enriched (depleted) water vapour. The wind vectors in Fig. 6 show that the changes in advection at the 850 hPa level cannot explain the change in $\delta^{18}O_v$. Interestingly the highest wind anomalies are found in the "2012" experiment, which is also the experiment that displayed a more widespread and regional isotopic response to sea ice changes. The slight increase in local wind anomalies could indicate that advection is responsible for the larger spatial extent of the isotopic response.

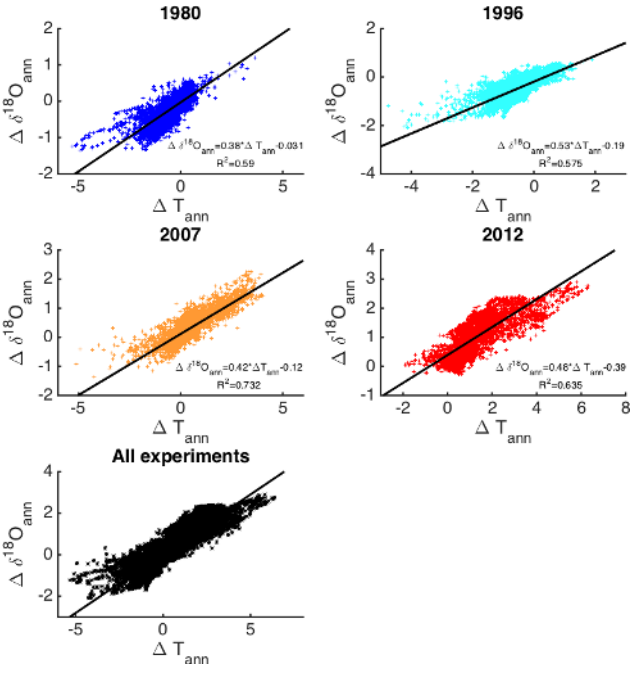

Figure 5. Scatter plots of anomalies of annual mean surface temperature (ΔT) vs. $\Delta\delta^{18}O_p$ anomalies. The plots show scatter plots of all grid points from 60 to 90° N for the different experiments compared to CTRL. The colours refer to the different experiments. Dark blue refers to experiment "1980", light blue to experiment "1996", orange to experiment "2007" and red to experiment "2012". Black colours show results from all experiments. Note that the scale of the x and y axes are different for each plot.

Changes in local evaporation here are investigated based on the surface latent heat flux over ocean and ice. To compare how changes in sea surface conditions change the amount of total local evaporation, only locations with grid points of strongly reduced sea ice (change bigger than 20 %) were selected and the amount of total latent heat flux per year for all grid points between 60 and 90° N was calculated for all experiments. To account for different numbers of grid points

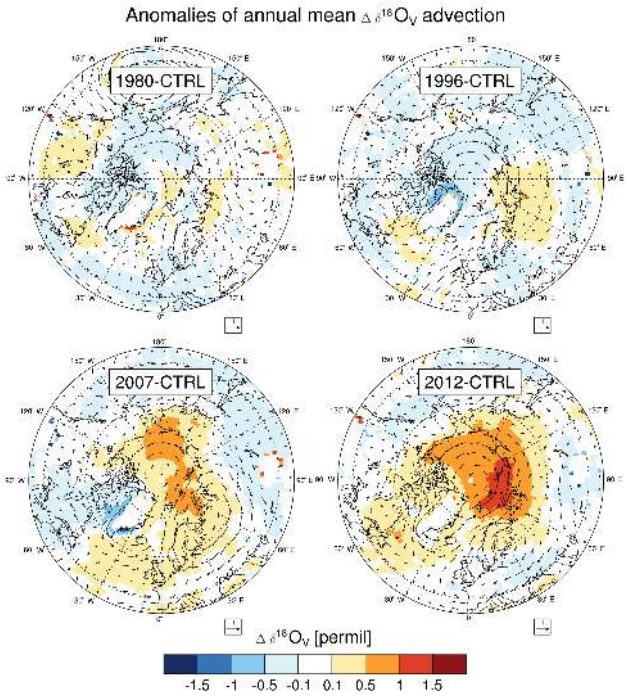

Figure 6. Annual mean anomalies of $\delta^{18}O_v$. Anomalies for the four simulations compared to the CTRL run. The arrows show the wind anomalies between the experiments and the CTRL run at the 850 hPa level.

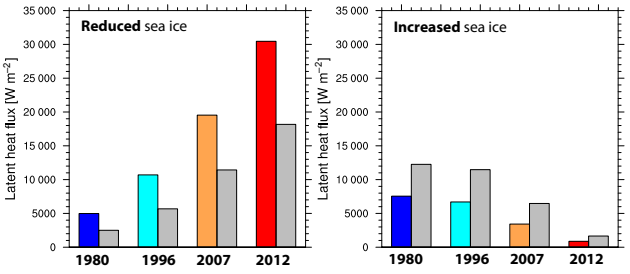

Figure 7. Latent heat flux for sea ice changes. Grid points of strongly reduced sea ice (anomaly bigger than 20 %) in each experiment were compared to identical grid points in the CTRL run and the amount of total latent heat flux per year for all grid points between 60 and 90° N was calculated for both experiments and the CTRL run. The same was done for grid points of strongly increased sea ice. The coloured bars represent the latent heat flux over sea ice change regions for the different experiments and the grey bars adjacent to the coloured bar represent the latent heat flux for the identical grid points in the CTRL run.

with sea ice change for each experiment, the comparison to the CTRL run is done using identical locations of the grid points, such that non-local effects in evaporation changes were excluded. As observed in Fig. 7 the amount of local evaporation is remarkably stronger for grid points where sea ice is reduced and weaker where sea ice is increased. The number of grid points of reduced sea ice in each of the experiments are 1980: 217, 1996: 444, 2007: 1148, 2012: 2116 and the number of grid points of increased sea ice are 1980: 1508, 1996: 1024, 2007:554, 2012: 437.

The two experiments with low sea ice extent ("2007" and "2012") have warmer temperatures, more intense evaporation and higher values of $\delta^{18}O_v$ than the CTRL experiment. This contrasts the two remaining experiments ("1980" and "1996"), which have sea ice extent larger than the CTRL run (based on 1979–2012 mean). In these experiments lower temperatures are observed as well as less intense evaporation and lower values of $\delta^{18}O_v$ compared to the CTRL experiment. Our results confirm that sea ice concentration and SST control the ability of the ocean to evaporate water.

4 Discussion

For isoCAM3, it is found that changes in sea ice and SSTs yield local changes in the δ^{18}O of Arctic precipitation. The isotopic response is sensitive to the spatial configuration of the sea surface conditions and the response of the changes are primarily local. Differences in the isotopic response in Greenland and the rest of the Arctic thus exist for both vapour and precipitation. The experiments show no changes of δ^{18}O for Greenland precipitation. Investigation of the vertical distribution of $\delta^{18}O_v$ anomalies are shown in Figs. 8 and 9. The zonal vertical cross sections of temperature and $\delta^{18}O_v$ along the latitude 77 °N show that the changes in the $\delta^{18}O_v$ and temperature are surface-based signals. This is also found in the spatial fields of $\delta^{18}O_v$ at different pressure levels in the vertical (see Appendix A). The precipitation anomalies are not occurring together with anomalies in the mid-troposphere $\delta^{18}O_v$ as seen in the vertical meridional cross sections of $\delta^{18}O_v$ (not shown). While the anomalies of vapour and precipitation at the same location do not have to be linked, it still suggest that the anomalies of precipitation are not connected to changes in air masses and large-scale transport but rather to local changes.

4.1 Are the moisture sources changing?

Based on the pronounced local structure of the isotopic response, and the evidence of an increase in ocean evaporation when sea ice is reduced and SSTs are warmed (see Fig. 7), it is speculated that the perturbation in the isotopic composition are caused by changes in the contribution from local moisture sources. An increase in local Arctic Ocean evaporation would contribute with heavily enriched water to the ambient vapour resulting in vapour that has a higher value of $\delta^{18}O_v$. This could explain the simulated $\delta^{18}O_v$ anomalies. In the case of an increased sea ice cover, the decrease in the contribution of local enriched water would result in ambient vapour with a lower value of $\delta^{18}O_v$. This hypothesis is supported by observational studies of the impact of Arctic sea

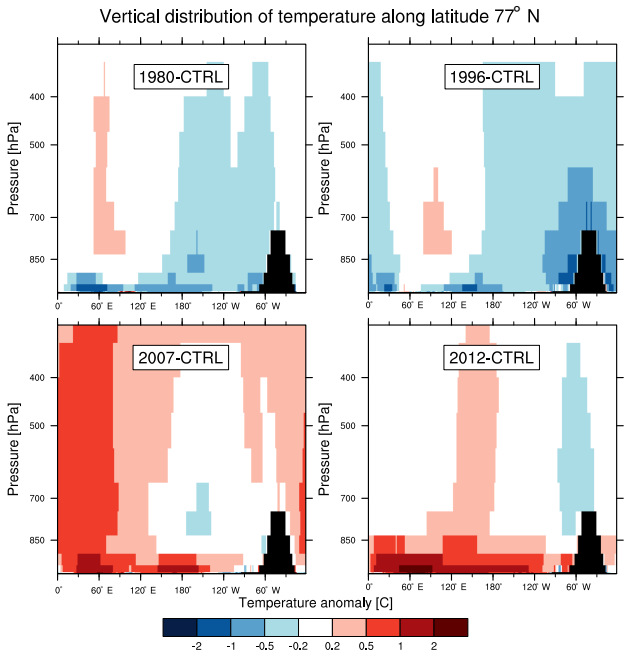

Figure 8. Vertical distribution of annual mean anomalies of temperature at the latitude band, 77° N. Annual mean anomalies for the four simulations compared to the CTRL run. Red and yellow colours represent an increase in temperature compared to the CTRL run. Blue colours represent a decrease in temperature compared to the CTRL run. The topography of Greenland is shown in black.

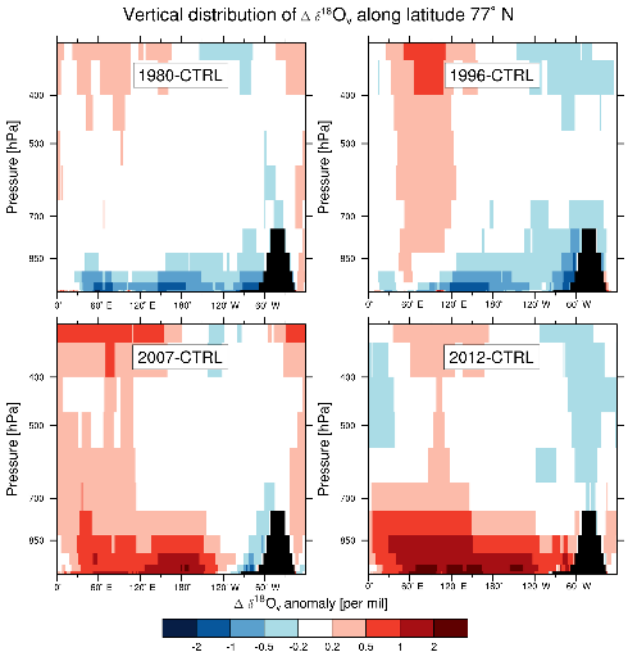

Figure 9. Vertical distribution of annual mean anomalies of δ^{18}O of vapour ($\delta^{18}O_v$) at the latitude band, 77° N. Annual mean anomalies for the four simulations compared to the CTRL run. Red and yellow colours represent an increase in $\delta^{18}O_p$ compared to the CTRL run. Blue colours represent a decrease in $\delta^{18}O_p$ compared to the CTRL run. The topography of Greenland is shown in black.

ice changes on the isotopic composition of moisture (Klein et al., 2015; Kopec et al., 2016). Changes in evaporation of local ocean water have also been suggested by modelling studies as important for sea ice induced changes in $\delta^{18}O_p$ (Sime et al., 2013; Noone, 2004). Furthermore, an analysis of future warming in the Arctic using state-of-the-art climate models showed changes in the hydrological cycle due to Arctic warming and sea ice changes (Bintanja and Selten, 2014). In that study it was found that moisture inflow from lower latitudes played a minor role, and the changes in the hydrological cycle were mainly caused by strongly intensified local surface evaporation.

An alternative explanation for the simulated changes in $\delta^{18}O_v$ and $\delta^{18}O_p$ is that the changes occur as result of changes in air mass characteristics. Reductions in the poleward temperature gradient would reduce the cooling and condensation that air masses experience during the northward transport. This would cause isotopic composition of the air masses to be less depleted. In this study, the sea surface conditions effect on Arctic warming is clearly seen on the simulated $T_{2\,m}$ (see Fig. 3). Additionally, also the vertical cross sections (Figs. 8 and 9) cannot exclude that the changes in the $\delta^{18}O_v$ are caused by changes in atmospheric temperature. Nevertheless, it is difficult to explain the spatially very local effects of $\delta^{18}O_p$ as a cause of reduction in the poleward temperature gradient. Yet, sea ice changes are connected to regions of cyclogenesis (Vihma, 2014; Bader et al., 2011). Thus, regions of open and warmer ocean surfaces might potentially steer cyclones to follow these paths and precipitate over the these regions, thereby creating a local signal of $\delta^{18}O_p$ changes. Our experimental design cannot reveal the synoptical variability and the effects of changed wind patterns are not clear from analysis of annual mean advection in the 850 hPa layer in Fig. 6. The wind speed ($\sqrt{u^2+v^2}$) at the 300 hPa level is weakened at midlatitudes in this study, which indicates that the changes in sea surface conditions are influencing atmospheric circulation, yet no clear connection to the changes in sea ice extent is found. Based on the considerations above it is difficult to separate the effects of changes in temperature and changes in evaporation, and consequently model simulations with moisture tracking features are suggested for further investigation of this study. However, independent of the cause of the changes, it is found that changes in sea surface conditions are important for the isotopic composition of non-Greenland $\delta^{18}O_p$ in the Arctic.

4.2 Influence on Greenland precipitation

Changes in the isotopic composition of Greenland precipitation are of special interest due to the ice core research sites in this region. Interestingly, none of the sea ice perturbation experiments in this study display $\delta^{18}O_p$ changes over Green-

land. Thus, the vertical distributions of T and $\delta^{18}O_v$ near the location of the ice core drilling site NEEM, Greenland ($\sim 77°$ N, 51° E), are used to investigate the differences in the response in Greenland and the rest of the Arctic. Figures 8 and 9 show the circumpolar zonal vertical distribution of T and $\delta^{18}O_v$ at the nearest grid point levels to NEEM. At non-Greenland locations the anomalies of T and $\delta^{18}O_v$ are surface-based signals, sensitive to the local conditions. However, near NEEM, the Baffin Bay sea ice extent and associated simulated response in $\delta^{18}O_v$ are important for the $\delta^{18}O_v$ at NEEM. In experiment "2007" the Baffin Bay sea ice extent is increased compared to the mean values, while the near-NEEM $\delta^{18}O_v$ displays negative anomalies of $\delta^{18}O_v$ in the range 0.2–1 ‰, this in spite of an overall Arctic enrichment. This suggests that the local conditions at Baffin Bay, and not the general Arctic conditions, are relevant for studying the $\delta^{18}O_v$ response to sea ice changes at NEEM. Modern observations of the isotopic composition of snow and water vapour from NEEM also show that variations in modern values of $\delta^{18}O$ correlate with conditions in Baffin Bay sea ice extent (Steen-Larsen et al., 2011).

The lack of sensitivity of the Greenland $\delta^{18}O_p$ to changes in Arctic Ocean surface conditions is argued to be related to the topography of Greenland. Specifically, the steep slopes of the ice sheet margin are associated with substantial orographic enhancement of precipitation and depletion of air mass water vapour content. Processes controlling the Greenland $\delta^{18}O_p$ might be decoupled from the processes influencing the $\delta^{18}O_p$ over the Arctic ocean. The Greenland katabatic wind blocking effect (Noël et al., 2014) might also play a role in blocking of low level moisture to Greenland.

We note that our experiment does not exhibit the strong warming observed over Greenland in 2012. The observed 2012 Greenland melting was attributed to the following key factors: the North American heat wave, transitions in the Arctic Oscillation and transport of warm air and vapour via an atmospheric river (Neff et al., 2014; Bonne et al., 2014). Forcing the model with only oceanic conditions can thus not create a similar atmospheric-induced warming.

In contrast to the results of this study, Sime et al. (2013) simulated 2–3 ‰ changes in central Greenland $\delta^{18}O_p$ for extremely warm climates with SST and sea ice conditions created from a coupled model experiment forced by large increases in CO_2. The main differences between the simulations in this study and in the study by Sime et al. (2013) are related to the distribution and magnitude of sea ice and SST changes especially near northern Greenland.

In the study by Sime et al. (2013) sea ice and SST changes also occur in the region north of Greenland. Also the magnitude of Arctic SST anomalies are 8–10 °C whereas the simulations in this study have anomalies of 3–5 °C. These differences are compelling as our experiment "2012" with the largest prescribed SST anomalies and sea ice changes is also the only experiment that simulates a regional isotopic response. This indicates that the magnitude of SST changes might control not only the amount of local evaporation, but also the regional extent of the isotopic response. Hence, it is possible that the simulated changes of $\delta^{18}O_p$ by Sime et al. (2013) have a regional extent due to the same reasons as experiment "2012".

Warming of the lower troposphere and associated weakening of the inversion layer might be important in controlling the extent of the isotopic response. As sea ice removal is connected to intense warming of the lower troposphere (Screen et al., 2012; Deser et al., 2010), it could be speculated that this warming is controlling the extent of the isotopic response. This would be possible as a weaker inversion layer allows atmospheric convection, and Abbot and Tziperman (2008) have shown that this can occur at high-latitudes in sea-ice-free regions in winter. Further investigation of the mechanism causing this change requires further idealised experiments following a similar design to Noone (2004), so that a systematic investigation of the atmospheric processes influencing the isotopic composition of moisture is possible.

5 Conclusions

The aim of this study was to investigate whether changes in sea ice and SSTs derived from observed anomalies can influence the isotopic composition of precipitation in the Arctic. Results are presented from isoCAM3 an isotope-equipped AGCM, forced with different distributions of Arctic sea ice changes and associated SST from the ERA-interim reanalysis product. These simulations show that changes in sea ice and sea surface conditions influence the isotopic composition of Arctic precipitation with regional changes of $\delta^{18}O_p$ of up to 3 ‰ in the Barents Sea region. However, no changes are found for Greenland: a region relevant for isotope records from ice cores. For all experiments it is found that regions of increased (decreased) sea ice extent and concentration result in enriched (depleted) $\delta^{18}O$ values of precipitation.

The $\delta^{18}O$ response to the ocean conditions is primarily local. Changes in sea ice and SSTs yield local surface-based anomalies of $\delta^{18}O$ of vapour. Differences in the isotopic response in Greenland and the rest of the Arctic thus exist for both vapour and precipitation. Within the same experiment large changes in $\delta^{18}O$ are observed over some regions and no changes over other regions. The geographical variations in the $\delta^{18}O$ response to changes in Arctic sea surface conditions show that the isotopic composition of Arctic precipitation is sensitive to the spatial distribution of the sea ice and SST changes, however not at Greenland. This means that different distributions of similar sea ice areas can produce very different $\delta^{18}O_p$ values at the same location. Or conversely, that different locations respond very differently in $\delta^{18}O_p$ to the same total Arctic sea ice extent. The isotopic composition of Greenland precipitation is unaffected by the imposed changes in the central Arctic sea ice cover in all experiments. Only conditions near Baffin Bay influence Greenland. As

many ice cores originate from the Greenland Ice Sheet this is an important result for the interpretation of isotope records.

Previous studies have shown that large changes in the state of sea ice and SST conditions influence the isotope composition over Greenland (Sime et al., 2013) and Antarctica (Noone, 2004) but this study is the first model experiment to show that minor (relative to Sime et al., 2013) perturbation in the sea ice cover and SST under present-day climate conditions can yield significant changes in the isotopic composition of precipitation in the Arctic, while at the same time not changing conditions in Greenland.

Data availability. The model output of the global simulations that provided the foundation for this study are available for other users. Due to the large file sizes, file transfer of these model outputs are available upon request to the author.

Appendix A

Annual mean $\delta^{18}O_p$ for the CTRL run is compared to observations of present-day annual mean $\delta^{18}O$ from Greenland ice cores (Vinther et al., 2010). Figure A1 shows that the iso-CAM3 model has an annual mean positive bias of $\delta^{18}O$.

No change in annual mean precipitation is found for each of the experiments compared to the CTRL run as shown in Fig. A2.

The spatial distributions of the anomalies of $\delta^{18}O_v$ at the 950 hPa level and 700 hPa level (Figs. A3 and A4) show that the anomalies of $\delta^{18}O_v$ are mostly found at surface levels for the entire Arctic region.

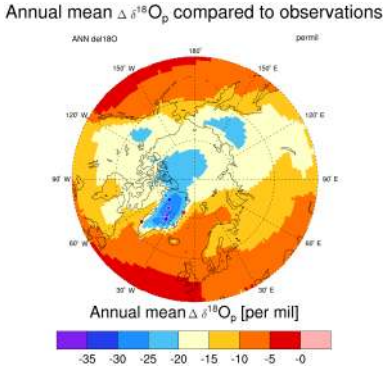

Figure A1. Annual mean $\delta^{18}O_p$ for the CTRL run compared to observations. The circles represent annual mean values from ice core and GNIP observations.

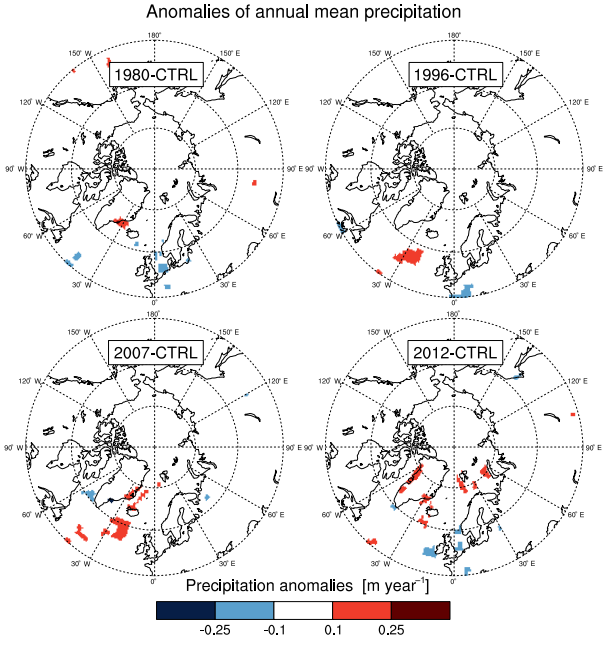

Figure A2. Annual mean anomalies of precipitation. Anomalies for the four simulations compared to the CTRL run.

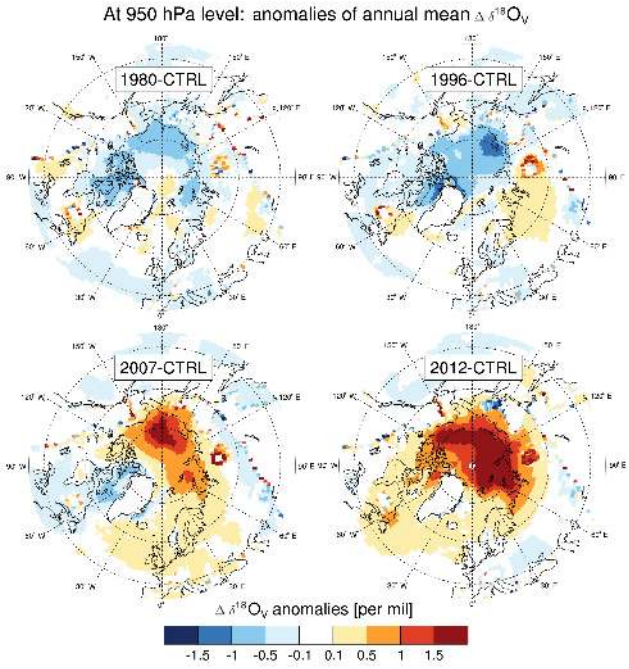

Figure A3. Annual mean anomalies of $\delta^{18}O_v$. Anomalies for the four simulations compared to the CTRL run. The arrows show the wind anomalies between the experiments and the CTRL run at the 950 hPa level.

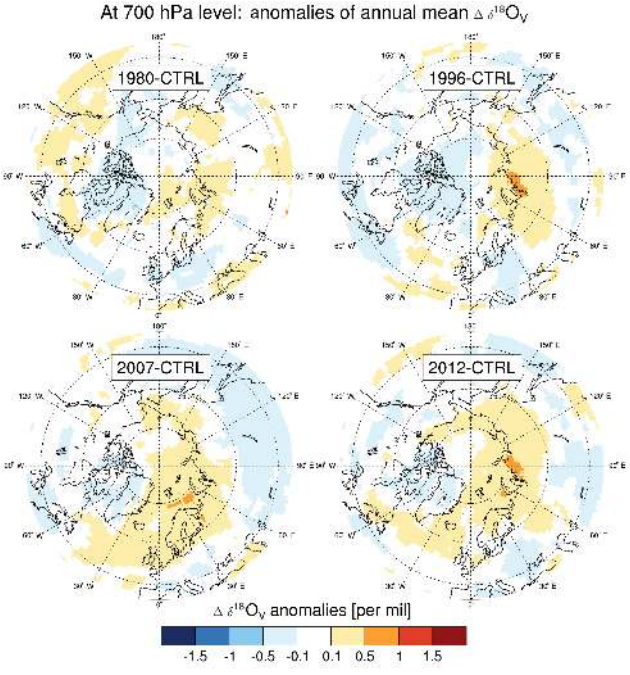

Figure A4. Annual mean anomalies of $\delta^{18}O_v$. Anomalies for the four simulations compared to the CTRL run. The arrows show the wind anomalies between the experiments and the CTRL run at the 700 hPa level.

Competing interests. The authors declare that they have no conflict of interest.

Acknowledgements. We thank the two anonymous reviewers for helpful comments and suggestions. The research leading to these results has received funding from the European Research Council under the European Union's Seventh Framework Programme (FP7/2007-2013)/ERC grant agreement number 610055 as part of the ice2ice project. The authors acknowledge the support of the Danish National Research Foundation through the Centre for Ice and Climate, Niels Bohr Institute.

Edited by: T. Röckmann
Reviewed by: two anonymous referees

References

Abbot, D. S. and Tziperman, E.: Sea ice, high-latitude convection, and equable climates, Geophys. Res. Lett., 35, L03702, doi:10.1029/2007GL032286, 2008.

Bader, J., Mesquita, M. D. S., Hodges, K. I., Keenlyside, N., Osterhus, S., and Miles, M.: A review on Northern Hemisphere sea-ice, storminess and the North Atlantic Oscillation: observations and projected changes, Atmos. Res., 101, 809–834, 2011.

Bintanja, R. and Selten, F.: Future increases in Arctic precipitation linked to local evaporation and sea-ice retreat, Nature, 509, 479–482, 2014.

Blüthgen, J., Gerdes, R., and Werner, M.: Atmospheric response to the extreme Arctic sea ice conditions in 2007, Geophys. Res. Lett., 39, L02707, doi:10.1029/2011GL050486, 2012.

Bonne, J.-L., Masson-Delmotte, V., Cattani, O., Delmotte, M., Risi, C., Sodemann, H., and Steen-Larsen, H. C.: The isotopic composition of water vapour and precipitation in Ivittuut, southern Greenland, Atmos. Chem. Phys., 14, 4419–4439, doi:10.5194/acp-14-4419-2014, 2014.

Budikova, D.: Role of Arctic sea ice in global atmospheric circulation: A review, Global Planet. Change, 68, 149–163, doi:10.1016/j.gloplacha.2009.04.001, 2009.

Collins, W. D., Rasch, P. J., Boville, B. A., Hack, J. J., McCaa, J. R., Williamson, D. L., Briegleb, B. P., Bitz, C. M., Lin, S.-J. J., and Zhang, M. H.: The formulation and atmospheric simulation of the Community Atmosphere Model version 3 (CAM3), J. Climate, 19, 2144–2161, doi:10.1175/JCLI3760.1, 2006.

Dansgaard, W.: Stable Isotopes in Precipitation, Tellus, 16, 436–468, doi:10.1111/j.2153-3490.1964.tb00181.x, 1964.

Dee, D. P., Uppala, S. M., Simmons, A. J., Berrisford, P., Poli, P., Kobayashi, S., Andrae, U., Balmaseda, M. A., Balsamo, G., Bauer, P., Bechtold, P., Beljaars, A. C. M., van de Berg, L., Bidlot, J., Bormann, N., Delsol, C., Dragani, R., Fuentes, M., Geer, A. J., Haimberger, L., Healy, S. B., Hersbach, H., Holm, E. V., Isaksen, L., Kallberg, P., Koehler, M., Matricardi, M., McNally, A. P., Monge-Sanz, B. M., Morcrette, J. J., Park, B. K., Peubey, C., de Rosnay, P., Tavolato, C., Thepaut, J. N., and Vitart, F.: The ERA-Interim reanalysis: configuration and performance of the data assimilation system, Q. J. Roy. Meteor. Soc., 137, 553–597, 2011.

Deser, C., Tomas, R., Alexander, M., and Lawrence, D.: The seasonal atmospheric response to projected Arctic sea ice loss in the late twenty-first century, J. Climate, 23, 333–351, 2010.

Divine, D., Isaksson, E., Martma, T., A. J. Meijer, H., Moore, J., Pohjola, V., van de Wal, R. S., and Godtliebsen, F.: Thousand years of winter surface air temperature variations in Svalbard and northern Norway reconstructed from ice-core data, Polar Res., 30, 1–12, doi:10.3402/polar.v30i0.7379, 2011.

Fauria, M. M., Grinsted, A., Helama, S., Moore, J., Timonen, M., Martma, T., Isaksson, E., and Eronen, M.: Unprecedented low twentieth century winter sea ice extent in the Western Nordic Seas since AD 1200, Clim. Dynam., 34, 781–795, 2010.

Fetterer, F., Knowles, K., Meier, W., and Savoie, M.: Sea ice index v.1, Natl. Snow and Ice Data Center, Boulder, CO), v2.1 available at: http://nsidc.org/data/G02135 (last access: 10 May 2017), 2002.

Johnsen, S. J., Dansgaard, W., and White, J. W. C.: The origin of Arctic precipitation under present and glacial conditions, Tellus B, 41, 452–468, doi:10.1111/j.1600-0889.1989.tb00321.x, 1989.

Klein, E. S., Cherry, J., Young, J., Noone, D., Leffler, A., and Welker, J.: Arctic cyclone water vapor isotopes support past sea ice retreat recorded in Greenland ice, Scientific reports, 5, 2015.

Kopec, B. G., Feng, X., Michel, F. A., and Posmentier, E. S.: Influence of sea ice on Arctic precipitation, P. Natl. Acad. Sci. USA, 113, 46–51, 2016.

Ku, M., Monaghan, A. J., Battisti, D. S., Küttel, M., Steig, E. J., Ding, Q., Monaghan, A. J., Battisti, D. S., Ku, M., Monaghan, A. J., and Battisti, D. S.: Seasonal climate information preserved in West Antarctic ice core water isotopes: Relationships to temperature, large-scale circulation, and sea ice, Clim. Dynam., 39, 1841–1857, doi:10.1007/s00382-012-1460-7, 2012.

Li, C., Battisti, D. S., and Bitz, C. M.: Can North Atlantic Sea Ice Anomalies Account for Dansgaard-Oeschger Climate Signals?*, J. Climate, 23, 5457–5475, 2010.

Liu, Z., Carlson, A. E., He, F., Brady, E. C., Otto-Bliesner, B. L., Briegleb, B. P., Wehrenberg, M., Clark, P. U., Wu, S., Cheng, J., Zhang, J., Noone, D., and Zhu, J.: Younger Dryas cooling and the Greenland climate response to CO_2, P. Natl. Acad. Sci., 109, 11101–11104, 2012.

Liu, Z., Wen, X., Brady, E. C., Otto-Bliesner, B., Yu, G., Lu, H., Cheng, H., Wang, Y., Zheng, W., Ding, Y., Others, Edwards, R. L., Cheng, J., Liu, W., and Yang, H.: Chinese cave records and the East Asia summer monsoon, Quaternary Sci. Rev., 83, 115–128, doi:10.1016/j.quascirev.2013.10.021, 2014.

Magnusdottir, G., Deser, C., and Saravanan, R.: The effects of North Atlantic SST and sea ice anomalies on the winter circulation in CCM3. Part I: Main features and storm track characteristics of the response, J. Climate, 17, 857–876, 2004.

Neff, W., Compo, G. P., Martin Ralph, F., and Shupe, M. D.: Continental heat anomalies and the extreme melting of the Greenland ice surface in 2012 and 1889, J. Geophys. Res.-Atmos., 119, 6520–6536, 2014.

Noël, B., Fettweis, X., van de Berg, W. J., van den Broeke, M. R., and Erpicum, M.: Sensitivity of Greenland Ice Sheet surface mass balance to perturbations in sea surface temperature and sea ice cover: a study with the regional climate model MAR, The Cryosphere, 8, 1871–1883, doi:10.5194/tc-8-1871-2014, 2014.

Noone, D.: Sea ice control of water isotope transport to Antarctica and implications for ice core interpretation, J. Geophys. Res., 109, D07105, doi:10.1029/2003JD004228, 2004.

Noone, D. and Sturm, C.: Comprehensive Dynamical Models of Global and Regional Water Isotope Distributions, Isoscapes: Understanding movement, pattern, and process on Earth through isotope mapping, p. 195, 2010.

Opel, T., Fritzsche, D., and Meyer, H.: Eurasian Arctic climate over the past millennium as recorded in the Akademii Nauk ice core (Severnaya Zemlya), Clim. Past, 9, 2379–2389, doi:10.5194/cp-9-2379-2013, 2013.

Pausata, F. S. R., Battisti, D. S., Nisancioglu, K. H., and Bitz, C. M.: Chinese stalagmite δ^{18}O controlled by changes in the Indian monsoon during a simulated Heinrich event, Nat. Geosci., 4, 474–480, doi:10.1038/ngeo1169, 2011.

Screen, J. A., Deser, C., and Simmonds, I.: Local and remote controls on observed Arctic warming, Geophys. Res. Lett., 39, L10709, doi:10.1029/2012GL051598, 2012.

Screen, J. A., Deser, C., Simmonds, I., and Tomas, R.: Atmospheric impacts of Arctic sea-ice loss, 1979–2009: separating forced change from atmospheric internal variability, Clim. Dynam., 43, 333–344, doi:10.1007/s00382-013-1830-9, 2013a.

Screen, J. A., Simmonds, I., Deser, C., and Tomas, R.: The Atmospheric Response to Three Decades of Observed Arctic Sea Ice Loss, J. Climate, 26, 1230–1248, doi:10.1175/JCLI-D-12-00063.1, 2013b.

Sewall, J. O. and Fricke, H. C.: Andean-scale highlands in the Late Cretaceous Cordillera of the North American western margin, Earth Planet. Sc. Lett., 362, 88–98, 2013.

Sime, L. C., Risi, C., Tindall, J. C., Sjolte, J., Wolff, E. W., Masson-Delmotte, V., and Capron, E.: Warm climate isotopic simulations: what do we learn about interglacial signals in Greenland ice cores?, Quaternary Sci. Rev., 67, 59–80, doi:10.1016/j.quascirev.2013.01.009, 2013.

Sjolte, J., Hoffmann, G., Johnsen, S. J., Vinther, B. M., Masson-Delmotte, V., and Sturm, C.: Modeling the water isotopes in Greenland precipitation 1959–2001 with the mesoscale model REMO-iso, J. Geophys. Res., 116, D18105, doi:10.1029/2010JD015287, 2011.

Sodemann, H., Masson-Delmotte, V., Schwierz, C., Vinther, B. M., and Wernli, H.: Interannual variability of Greenland winter precipitation sources: 2. Effects of North Atlantic Oscillation variability on stable isotopes in precipitation, J. Geophys. Res.-Atmos., 113, 1–21, doi:10.1029/2007JD009416, 2008a.

Sodemann, H., Schwierz, C., and Wernli, H.: Interannual variability of Greenland winter precipitation sources: Lagrangian moisture diagnostic and North Atlantic Oscillation influence, J. Geophys. Res.-Atmos., 113, D03107, doi:10.1029/2007JD008503, 2008b.

Speelman, E. N., Sewall, J. O., Noone, D., Huber, M., der Heydt, A. V., Damsté, J. S., Reichart, G.-J., von der Heydt, A., Damsté, J. S., and Reichart, G.-J.: Modeling the influence of a reduced equator-to-pole sea surface temperature gradient on the distribution of water isotopes in the Early/Middle Eocene, Earth Planet. Sc. Lett., 298, 57–65, doi:10.1016/j.epsl.2010.07.026, 2010.

Steen-Larsen, H. C., Masson-Delmotte, V., Sjolte, J., Johnsen, S. J., Vinther, B. M., Bréon, F.-M., Clausen, H., Dahl-Jensen, D., Falourd, S., Fettweis, X., Gallée, H., Jouzel, J., Kageyama, M., Lerche, H., Minster, B., Picard, G., Punge, H. J., Risi, C., Salas, D., Schwander, J., Steffen, K., Sveinbjörnsdóttir, A. E., Svensson, A., and White, J.: Understanding the climatic signal in the water stable isotope records from the NEEM shallow firn/ice cores in northwest Greenland, J. Geophys. Res.-Atmos., 116, D06108, doi:10.1029/2010JD014311, 2011.

Sturm, C., Zhang, Q., and Noone, D.: An introduction to stable water isotopes in climate models: benefits of forward proxy modelling for paleoclimatology, Clim. Past, 6, 115–129, doi:10.5194/cp-6-115-2010, 2010.

Tharammal, T., Paul, A., Merkel, U., and Noone, D.: Influence of Last Glacial Maximum boundary conditions on the global water isotope distribution in an atmospheric general circulation model, Clim. Past, 9, 789–809, doi:10.5194/cp-9-789-2013, 2013.

Vihma, T.: Effects of Arctic sea ice decline on weather and climate: A review, Surv. Geophys., 35, 1175–1214, 2014.

Vinther, B. M., Jones, P. D., Briffa, K. R., Clausen, H. B., Andersen, K. K., Dahl-Jensen, D., and Johnsen, S. J.: Climatic signals in multiple highly resolved stable isotope records from Greenland, Quaternary Sci. Rev., 29, 522–538, doi:10.1016/j.quascirev.2009.11.002, 2010.

White, J. W. C., Barlow, L. K., Fisher, D., Grootes, P., Jouzel, J., Johnsen, S. J., Stuiver, M., and Clausen, H.: The climate signal in the stable isotopes of snow from Summit, Greenland: Results of comparisons with modern climate observations, J. Geophys. Res.-Oceans, 102, 26425–26439, 1997.